Numerical Experiments with the Fokker-Planck Equation in 1D Slab Geometry

Óscar López Pouso*
Nizomjon Jumaniyazov†

January 9, 2016

Abstract

Several numerical experiments with the steady monoenergetic Fokker-Planck equation in the 1D slab are performed and discussed. Planar-geometry symmetry is assumed. Results are obtained with a new numerical scheme of order 2 based on finite differences.

MSC 2010: 35Q84, 65-05, 65Z05, 78M20, 78A35, 35K65.
Keywords: Fokker-Planck equation, finite differences, Crank-Nicolson scheme, two-way diffusion equations, continuous scattering operator.

1 Introduction

The goal of this paper is to compute the function

$$\psi : (\mu, z) \in Q = [-1, 1] \times [Z_{\text{ini}}, Z_{\text{fin}}] \to \psi(\mu, z) \in \mathbb{R},$$

understanding that $Z_{\text{ini}}, Z_{\text{fin}} \in \mathbb{R}$, $Z_{\text{ini}} < Z_{\text{fin}}$, and that ψ is the solution of the problem defined by the two-way (also, forward-backward) diffusion PDE

$$\mu \frac{\partial \psi}{\partial z} + \alpha\psi - \sigma \frac{\partial}{\partial \mu}\left[\left(1 - \mu^2\right) \frac{\partial \psi}{\partial \mu} \right] = W \text{ for } (\mu, z) \in Q \tag{1}$$

and the incoming flux boundary conditions

$$\psi(\mu, Z_{\text{ini}}) = f(\mu) \text{ for } \mu \in (0, 1], \tag{2}$$

$$\psi(\mu, Z_{\text{fin}}) = g(\mu) \text{ for } \mu \in [-1, 0). \tag{3}$$

*Departamento de Matemática Aplicada, Facultad de Matemáticas, Universidad de Santiago de Compostela. C/ Lope Gómez de Marzoa s/n, Campus Vida, 15782 Santiago de Compostela (A Coruña, Spain). Email: oscar.lopez@usc.es.

†Department of Applied Mathematics and Mathematical Physics, Urgench State University, Urgench 220100 (Uzbekistan). Email: nizomjon_jumaniyazov@yahoo.com.

In Equation (1), $\alpha \geq 0$, $\sigma > 0$ and W are given functions of $(\mu, z) \in Q$, while f and g in Equations (2) and (3) are given functions of μ in $(0, 1]$ and in $[-1, 0)$, respectively.

From the nuclear engineering viewpoint, Equations (1)–(3) represent the well-known Fokker-Planck problem in 1D slab with planar-geometry symmetry. The fact that the $\mu = 0$ extreme is open in conditions (2) and (3) as well as the absence of boundary conditions at $|\mu| = 1$ can be explained by physical considerations; details are given in Section 4. From the mathematical viewpoint, there are also analytical reasons that support the well-posedness of Problem (1)–(3) in many particular cases; the interested reader might like to consult references [1], [2], [3], [4], [7], [8], and [9]. In particular, the absence of boundary conditions at $|\mu| = 1$ is related to the degeneracy of the inner diffusion coefficient $1 - \mu^2$ at $|\mu| = 1$.

When designing a numerical scheme, it is much convenient to bear in mind a paradigm of the solution, and this includes to have information about its regularity. To the authors' knowledge, there is no reference that proves regularity of the solution in the classical C^k setting, but in [9], which studies Problem (1)–(3) with $\alpha \equiv W \equiv 0$ and σ constant, the authors talk about this question in the following terms:[(a)] "The numerical results suggest that, in general, $f(0, \mu)$ and $f(1, \mu)$ are continuous at $\mu = 0$, but that $f_\mu(0, \mu)$ is singular as $\mu \to 0^-$, while $f_\mu(1, \mu)$ is singular as $\mu \to 0^+$." In this line, which is in accordance with all the available numerical results, we are going to look for a solution ψ which is continuous on the compact rectangle Q, remembering that it could be non-differentiable even for constant data functions. Somewhat hidden in this posture is the conjecture that diffusivity makes ψ be continuous for a large class of data functions (in contrast, ψ is easily discontinuous when $\sigma \equiv 0$).

Inasmuch as Equations (2) and (3) imply that

$$f \in \mathrm{C}((0, 1]), \ g \in \mathrm{C}([-1, 0)), \text{ and} \tag{4}$$

$$\text{both } \lim_{\mu \downarrow 0} f(\mu) \text{ and } \lim_{\mu \uparrow 0} g(\mu) \text{ must exist in } \mathbb{R} \tag{5}$$

so that a continuous solution ψ exists, it will be assumed throughout this paper that conditions (4) and (5) are fulfilled, and the notations $f(0)$ and $g(0)$ will be used with their obvious meanings. This amounts to say that f and g are supposed to be continuous on $[0, 1]$ and on $[-1, 0]$, respectively.

There are two former papers that connect with this one in a special fashion: Vanaja [10] proposes, for $\alpha \equiv W \equiv 0$ and σ constant, a finite difference scheme of order one, and Kim and Tranquilli [6] employ separation of variables and variation of parameters to solve the problem when α and σ may depend on z (but not on μ) and $W \equiv 0$. We connect with [10] because ours is also a finite difference scheme, and we take profit of the graphical results in [6] to compare with our outcomes.

[(a)] In [9], f is our ψ, $Z_{\mathrm{ini}} = 0$ and $Z_{\mathrm{fin}} = 1$. Also, f_μ denotes $\frac{\partial \psi}{\partial \mu}$.

Section 2 is devoted to the derivation of the numerical scheme. In Section 3 a collection of numerical results is shown, and in particular the order 2 of the scheme is experimentally checked. Section 4 contains the physical essentials, and Section 5 the conclusions.

2 Numerical scheme

From the viewpoint of the numerical scheme, variable z is to be interpreted as time, and variable μ as space. This mental abstraction is helpful for establishing the analogies with the classical finite difference schemes employed for solving the evolutive 1D heat equation. Accordingly, the expressions *initial* and *final condition* will be used to make reference to Equations (2) and (3), respectively.

Let us call $Q_- = [-1, 0) \times [Z_{\text{ini}}, Z_{\text{fin}}]$, $Q_+ = (0, 1] \times [Z_{\text{ini}}, Z_{\text{fin}}]$, and $Q_0 = \{0\} \times [Z_{\text{ini}}, Z_{\text{fin}}]$. Let us also call $D(\mu) = 1 - \mu^2$.

We could say that we have a "final value problem" (FVP) determined by $g(\mu)$ on Q_- and an "initial value problem" (IVP) determined by $f(\mu)$ on Q_+. However, such an assertion may be misleading, as these two problems are not independent except in the trivial situation $\sigma \equiv 0$, which is not our case.

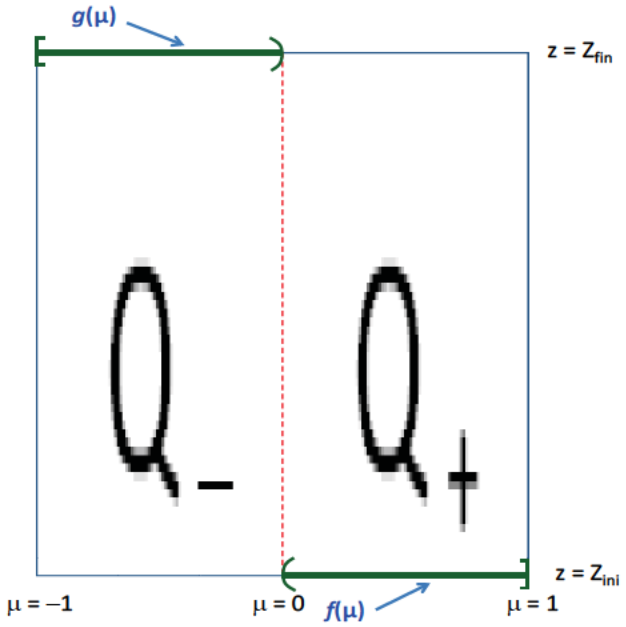

Figure 1: The thicker lines on the boundary of Q are marking out the set of points where the solution ψ is given by functions f and g.

Indeed, the presence of the diffusive term $\sigma \frac{\partial}{\partial \mu}\left[D(\mu)\frac{\partial \psi}{\partial \mu}\right]$ makes $\psi_{|Q_-}$ be dependent on $f(\mu)$ as well, and clearly a reciprocal comment holds

for $\psi_{|Q_+}$. Naturally, this exchange of information between Q_- and Q_+ affects the values of the solution at the points of Q_0 in such a way that it is not possible to know them in advance. We emphasize that, in case one desired to solve this problem (either on Q_- or on Q_+) in an "step by step" way, as it is done for solving the evolutive heat equation, the values on Q_0, which are unknown, would be required. On the other hand, it is also impossible to employ an "step by step" marching method on the whole Q, since $\psi_{|\{(\mu,Z_{\rm ini}):\ \mu\in[-1,0]\}}$ is left to go forward and $\psi_{|\{(\mu,Z_{\rm fin}):\ \mu\in[0,1]\}}$ is left to go backward.

Comments in the two paragraphs above are apparent when looking at Figure 1.

Consequently, one must rather think

- either of using an iterative process starting with an initial guess of the solution on Q_0,
- or of using a global scheme like those used for solving the two-dimensional Poisson equation, where the approximations at all mesh points (μ_i, z_n) are simultaneously obtained as the solution of a single large (but sparse) linear system.

In this paper, we have adopted the second approach. It seems that the first one would also work (see [10]), but we have not made comparisons between them so far.

Since it is also true that this is a problem with initial-final value structure, implicit numerical schemes should be able to solve it more robustly than explicit ones. Considering now that what it is written as implicit on the FVP half Q_- becomes explicit on the IVP half Q_+,[(b)] and vice versa, one concludes that a Crank-Nicolson-like scheme, possessing an implicit and an explicit part with the same weights, is a perfect candidate for being used on the whole grid without modifying the scheme's appearance. The details are as follows.

For given natural numbers I and N strictly greater than 1, let us consider the uniform meshes

$$\mu_i = -1 + (i-1)h \text{ for } i \in \{1,\dots,I\},\ \text{with } h = \Delta\mu = \frac{2}{I-1} \tag{6}$$

and

$$z_n = Z_{\rm ini} + (n-1)k \text{ for } k \in \{1,\dots,N\},\ \text{with } k = \Delta z = \frac{Z_{\rm fin} - Z_{\rm ini}}{N-1}. \tag{7}$$

Hence

$$\mu_1 = -1 < \mu_2 < \cdots < \mu_{I-1} < \mu_I = 1 \tag{8}$$

and

$$z_1 = Z_{\rm ini} < z_2 < \cdots < z_{N-1} < z_N = Z_{\rm fin}. \tag{9}$$

In the sequel, the following notations will be employed:

[(b)] Another way to say the same thing: on Q_- an implicit scheme must be written in "forward form", while on Q_+ the same scheme must be written in "backward form".

- For a given function $\mathscr{A}$ of μ, $\overline{\mathscr{A}}_i = \mathscr{A}(\mu_i)$ and $\overline{\mathscr{A}}_{i\pm\frac{1}{2}} = \mathscr{A}(\mu_i \pm \frac{h}{2})$.
- For a given function $\mathscr{B}$ of (μ, z), $\overline{\mathscr{B}}_i^n = \mathscr{B}(\mu_i, z_n)$.
- ψ_i^n will be the approximation of the unknown solution ψ at the mesh point (μ_i, z_n): $\psi_i^n \approx \psi(\mu_i, z_n) =: \overline{\psi}_i^n$.
- $z_{n+\frac{1}{2}} = z_n + \frac{k}{2}$.

2.1 Derivation of the numerical scheme

Firstly, one follows the Crank-Nicolson idea to get

$$\begin{aligned} & \mu_i \frac{\overline{\psi}_i^{n+1} - \overline{\psi}_i^n}{k} \overset{O(k^2)}{\approx} \mu_i \frac{\partial \psi}{\partial z}(\mu_i, z_{n+\frac{1}{2}}) \overset{O(k^2)}{\approx} \\ & \frac{\mu_i}{2}\left(\frac{\partial \psi}{\partial z}(\mu_i, z_n) + \frac{\partial \psi}{\partial z}(\mu_i, z_{n+1})\right). \end{aligned} \tag{10}$$

According to Equation (1),

$$\mu_i \frac{\partial \psi}{\partial z}(\mu_i, z_m) = \overline{W}_i^m - \overline{\alpha}_i^m \overline{\psi}_i^m + \overline{\sigma}_i^m \frac{\partial}{\partial \mu}\left[D(\mu)\frac{\partial \psi}{\partial \mu}\right]_{(\mu,z)=(\mu_i,z_m)} \tag{11}$$

for $m \in \{n, n+1\}$.

Finally, the diffusive term is discretized as follows:

1. If $i = 1$, it is useful to notice that $\overline{D}_1 = 0$, which allows one to proceed as follows (see for instance [5, p. 207]):

$$\frac{\partial}{\partial \mu}\left[D(\mu)\frac{\partial \psi}{\partial \mu}\right]_{(\mu,z)=(\mu_1,z_m)} \overset{O(h^2)}{\approx} \frac{4\overline{D}_2 \frac{\partial \psi}{\partial \mu}(\mu_2, z_m) - \overline{D}_3 \frac{\partial \psi}{\partial \mu}(\mu_3, z_m)}{2h} \tag{12}$$

and, for $r \in \{2, 3\}$, the standard centered formula of two points gives

$$\frac{\partial \psi}{\partial \mu}(\mu_r, z_m) \overset{O(h^2)}{\approx} \frac{\overline{\psi}_{r+1}^m - \overline{\psi}_{r-1}^m}{2h}. \tag{13}$$

2. If $i \in \{2, \ldots, I-1\}$, the standard second order centered formula gives

$$\begin{aligned} & \frac{\partial}{\partial \mu}\left[D(\mu)\frac{\partial \psi}{\partial \mu}\right]_{(\mu,z)=(\mu_i,z_m)} \overset{O(h^2)}{\approx} \\ & \frac{\overline{D}_{i-\frac{1}{2}}\overline{\psi}_{i-1}^m - \left(\overline{D}_{i-\frac{1}{2}} + \overline{D}_{i+\frac{1}{2}}\right)\overline{\psi}_i^m + \overline{D}_{i+\frac{1}{2}}\overline{\psi}_{i+1}^m}{h^2}. \end{aligned} \tag{14}$$

3. If $i = I$, the situation is analogous to that of $i = 1$. In this case, one takes advantage of the equality $\overline{D}_I = 0$ to write down

$$\begin{aligned} & \frac{\partial}{\partial \mu}\left[D(\mu)\frac{\partial \psi}{\partial \mu}\right]_{(\mu,z)=(\mu_I,z_m)} \overset{O(h^2)}{\approx} \\ & \frac{\overline{D}_{I-2}\frac{\partial \psi}{\partial \mu}(\mu_{I-2}, z_m) - 4\overline{D}_{I-1}\frac{\partial \psi}{\partial \mu}(\mu_{I-1}, z_m)}{2h} \end{aligned} \tag{15}$$

and, for $r \in \{I-2, I-1\}$, (13) is used again.

2.2 Description of the numerical scheme

The above differentiation formulas suggest, after some reordering, the following scheme, which is well-defined if $I \geq 4$, I even, and $N \geq 2$. As it will be seen, a correction must be done in order to use the scheme for $I > 4$, I odd.

- For $(i,n) \in \{1\} \times \{1,\dots,N-1\}$,

$$\left(-\frac{\mu_1}{k} + \frac{\overline{\alpha}_1^n}{2} + \frac{\overline{\sigma}_1^n \overline{D}_2}{2h^2}\right)\psi_1^n + \left(-\frac{\overline{\sigma}_1^n \overline{D}_3}{8h^2}\right)\psi_2^n + \left(-\frac{\overline{\sigma}_1^n \overline{D}_2}{2h^2}\right)\psi_3^n + \\ + \left(\frac{\overline{\sigma}_1^n \overline{D}_3}{8h^2}\right)\psi_4^n + \left(\frac{\mu_1}{k} + \frac{\overline{\alpha}_1^{n+1}}{2} + \frac{\overline{\sigma}_1^{n+1} \overline{D}_2}{2h^2}\right)\psi_1^{n+1} + \\ + \left(-\frac{\overline{\sigma}_1^{n+1} \overline{D}_3}{8h^2}\right)\psi_2^{n+1} + \left(-\frac{\overline{\sigma}_1^{n+1} \overline{D}_2}{2h^2}\right)\psi_3^{n+1} + \\ + \left(\frac{\overline{\sigma}_1^{n+1} \overline{D}_3}{8h^2}\right)\psi_4^{n+1} = \frac{\overline{W}_1^n + \overline{W}_1^{n+1}}{2}. \quad (16)$$

- For $(i,n) \in \{2,\dots,I-1\} \times \{1,\dots,N-1\}$,

$$\left(-\frac{\overline{\sigma}_i^n \overline{D}_{i-\frac{1}{2}}}{2h^2}\right)\psi_{i-1}^n + \left(-\frac{\mu_i}{k} + \frac{\overline{\alpha}_i^n}{2} + \frac{\overline{\sigma}_i^n \left(\overline{D}_{i-\frac{1}{2}} + \overline{D}_{i+\frac{1}{2}}\right)}{2h^2}\right)\psi_i^n + \\ + \left(-\frac{\overline{\sigma}_i^n \overline{D}_{i+\frac{1}{2}}}{2h^2}\right)\psi_{i+1}^n + \left(-\frac{\overline{\sigma}_i^{n+1} \overline{D}_{i-\frac{1}{2}}}{2h^2}\right)\psi_{i-1}^{n+1} + \\ + \left(\frac{\mu_i}{k} + \frac{\overline{\alpha}_i^{n+1}}{2} + \frac{\overline{\sigma}_i^{n+1} \left(\overline{D}_{i-\frac{1}{2}} + \overline{D}_{i+\frac{1}{2}}\right)}{2h^2}\right)\psi_i^{n+1} + \\ + \left(-\frac{\overline{\sigma}_i^{n+1} \overline{D}_{i+\frac{1}{2}}}{2h^2}\right)\psi_{i+1}^{n+1} = \frac{\overline{W}_i^n + \overline{W}_i^{n+1}}{2}. \quad (17)$$

- For $(i,n) \in \{I\} \times \{1,\dots,N-1\}$,

$$\left(\frac{\overline{\sigma}_I^n \overline{D}_{I-2}}{8h^2}\right)\psi_{I-3}^n + \left(-\frac{\overline{\sigma}_I^n \overline{D}_{I-1}}{2h^2}\right)\psi_{I-2}^n + \left(-\frac{\overline{\sigma}_I^n \overline{D}_{I-2}}{8h^2}\right)\psi_{I-1}^n + \\ + \left(-\frac{\mu_I}{k} + \frac{\overline{\alpha}_I^n}{2} + \frac{\overline{\sigma}_I^n \overline{D}_{I-1}}{2h^2}\right)\psi_I^n + \left(\frac{\overline{\sigma}_I^{n+1} \overline{D}_{I-2}}{8h^2}\right)\psi_{I-3}^{n+1} + \\ + \left(-\frac{\overline{\sigma}_I^{n+1} \overline{D}_{I-1}}{2h^2}\right)\psi_{I-2}^{n+1} + \left(-\frac{\overline{\sigma}_I^{n+1} \overline{D}_{I-2}}{8h^2}\right)\psi_{I-1}^{n+1} + \\ + \left(\frac{\mu_I}{k} + \frac{\overline{\alpha}_I^{n+1}}{2} + \frac{\overline{\sigma}_I^{n+1} \overline{D}_{I-1}}{2h^2}\right)\psi_I^{n+1} = \frac{\overline{W}_I^n + \overline{W}_I^{n+1}}{2}. \quad (18)$$

Correction for I odd. The number of unknowns is $I \times N$, and the number of equations in the scheme above is $I \times (N-1)$; moreover, the initial and final conditions from Equations (2) and (3) provides one with I values when I is even (they are $\psi_i^1 = \overline{f}_i$ for $i = \frac{I}{2}+1,\dots,I$ and $\psi_i^N = \overline{g}_i$ for $i = 1,\dots,\frac{I}{2}$), but with only $I-1$ values when I is odd (they are $\psi_i^1 = \overline{f}_i$ for $i = \frac{I+3}{2},\dots,I$ and $\psi_i^N = \overline{g}_i$ for $i = 1,\dots,\frac{I-1}{2}$). As a result,

the number of equations equals the number of unknowns when I is even, but there is one equation left when I is odd.

Consider I odd, and observe that $\mu_{\frac{I+1}{2}} = 0$. As a first approach (which will be improved below) one could think of using either the *numerical initial condition*

$$\psi^1_{\frac{I+1}{2}} = f(0) \tag{19}$$

or the *numerical final condition*

$$\psi^N_{\frac{I+1}{2}} = g(0). \tag{20}$$

This strategy, even when it has been tested with acceptable results, is asymmetric, since in fact the imposition of both conditions (19) and (20), and not only one of them, would be desirable. The reason is that we are looking for a continuous solution.

It is natural to proceed as follows. We are going to discard the $N-1$ equations corresponding to the choice $i = \frac{I+1}{2}$ in Equation (17),[(c)] to impose conditions (19) and (20), and to consider a new set of $N-2$ equations, for $\mu = 0$ and the z-nodes in the open interval $(Z_{\text{ini}}, Z_{\text{fin}})$, which will close the linear system. In order to obtain these new set of equations, simply notice that Equation (1) becomes, for $\mu = 0$, into

$$\alpha(0,z)\psi(0,z) - \sigma(0,z)\frac{\partial^2\psi}{\partial\mu^2}(0,z) = W(0,z) \text{ for } z \in [Z_{\text{ini}}, Z_{\text{fin}}]. \tag{21}$$

When thought in the open interval $(Z_{\text{ini}}, Z_{\text{fin}})$, Equation (21) suggests

$$\overline{\alpha}^n_{i^\star}\psi^n_{i^\star} - \overline{\sigma}^n_{i^\star}\frac{\psi^n_{i^\star-1} - 2\psi^n_{i^\star} + \psi^n_{i^\star+1}}{h^2} = \overline{W}^n_{i^\star} \quad \text{for } n \in \{2,\dots,N-1\}, \tag{22}$$

where $i^\star = \frac{I+1}{2}$. Equivalently,

$$\left(-\frac{\overline{\sigma}^n_{i^\star}}{h^2}\right)\psi^n_{i^\star-1} + \left(\overline{\alpha}^n_{i^\star} + \frac{2\overline{\sigma}^n_{i^\star}}{h^2}\right)\psi^n_{i^\star} + \left(-\frac{\overline{\sigma}^n_{i^\star}}{h^2}\right)\psi^n_{i^\star+1} = \overline{W}^n_{i^\star} \quad \text{for } n \in \{2,\dots,N-1\}. \tag{23}$$

To summarize: when I is odd, the $N-1$ equations corresponding to the choice $i = \frac{I+1}{2}$ in Equation (17) are discarded, and the following N equations are considered instead: Equation (19), Equation (20), plus the set of $N-2$ Equations (23).

Hereinafter, we shall use the expression "even-scheme" to mean the use of I even, and "odd-scheme" to mean the use of I odd.

3 Numerical results

Both the even and the odd-scheme have been implemented in MATLAB® (R2012b). As it was explained above, the approximate values ψ^n_i are obtained by solving a linear sparse system of dimension $I \times N$.

In this section:

[(c)] There is no reason to prefer removing the first one versus the last one of these. Therefore, we eliminate all of them and we follow an alternative line of action.

- $E_{\text{abs}}(Q) = \max_Q |\psi_{\text{grid}} - \psi|$, where ψ_{grid} is representing the approximate solution and the maximum is taken over the set of all nodes.
- $D_{\text{abs}}(Q) = \max_Q |\psi_{\text{coarse}} - \psi_{\text{fine}}|$ is the maximum punctual difference between a coarse-fine embedded pair of numerical approximations: the $(2I-1, 2N-1)$ fine grid is built by roughly doubling the (I, N) coarse grid in each variable. The maximum is taken over all common nodes, i. e., over all the nodes of the coarse grid.
- The (μ, z) column within the tables reports the grid point where the value of $E_{\text{abs}}(Q)$ or $D_{\text{abs}}(Q)$ on the left is attained.

Numerical results show that the (odd or even) scheme converges with the expected order 2 in both μ and z. Notice that this is an experimental assertion, as no numerical analysis has been carried out. The order and order* within the tables have been truncated after performing their computation with more decimals than those present in the error columns (consequently, if the reader does the operations employing the numbers as they occur in the tables, the result will differ slightly). In all our experiments, the odd-scheme has performed better than (or as good as) the even-scheme.

3.1 Test cases with known regular solution

Here, the adjective "regular" is being used as synonymous of "belonging to $\mathrm{C}^\infty(Q)$". Test cases with known regular solution are useful to check scheme's convergence and order. They are easily derived thanks to the presence of the source term W; the idea is to fix, freely, Z_{ini}, Z_{fin}, α and σ, as well as a function $\psi \in \mathrm{C}^\infty(Q)$ which is going to be the exact solution. The data functions left, namely W, f and g, are computed from Equations (1)–(3).

The following facts, which by the way are expected from the discretizations employed, will be observed for regular ψ (assertions about "the scheme" are valid for both the even and the odd-scheme):

1. The scheme solves the problem exactly if $\psi(\cdot, z)$ is a polynomial of degree ≤ 1 in μ and $\psi(\mu, \cdot)$ is a polynomial of degree ≤ 2 in z. See Table 1 in Subsection 3.1.1.
2. The scheme is exact with respect to z and converges with order $O(h^2)$ for constant k if $\psi(\mu, \cdot)$ is a polynomial of degree ≤ 2 in z. See Table 2 in Subsection 3.1.2.
3. The scheme is exact with respect to μ and converges with order $O(k^2)$ for constant h if $\psi(\cdot, z)$ is a polynomial of degree ≤ 1 in μ. See Table 3 in Subsection 3.1.2.
4. The scheme converges with order $O(h^2) + O(k^2)$. See Tables 4 and 5 in Subsection 3.1.3.

In the examples below, we consider $Z_{\text{ini}} = 0$, $Z_{\text{fin}} = 1$ and different combinations of

$$\alpha \in \{0, 1, |\sin(12\mu z)|, 2 + \sin(12\mu z)\} \tag{24}$$

and

$$\sigma \in \{1, 1 + \sin(12\mu z)\cos(12\mu z)\}. \tag{25}$$

3.1.1 Test case with known regular solution #1

If the exact solution is $\psi(\mu, z) = \mu z^2$, then the method is exact, and only round-off errors occur. For all possible combinations of (24) and (25) the maximum error is less than 10^{-15} when $I = 11$ and $N = 10$. Table 1 shows the error for one of these combinations. Notice that round-off error is added when I and N increase.

(I, N)	$E_{\text{abs}}(Q)$
$(11, 10)$	3.88×10^{-16}
$(101, 91)$	5.22×10^{-15}
$(1001, 901)$	2.50×10^{-13}

Table 1: Numerical results for the test case with exact solution $\psi(\mu, z) = \mu z^2$, for $\alpha(\mu, z) = |\sin(12\mu z)|$ and $\sigma(\mu, z) = 1 + \sin(12\mu z)\cos(12\mu z)$.

3.1.2 Test cases with known regular solution #2

If the exact solution is $\psi(\mu, z) = \mu^2 z^2$, then the method is exact with respect to z, and hence high accuracy can be reached by refining only the μ-mesh, i. e., by augmenting I while maintaining N constant. In this case, the effect of increasing the value of N is to add round-off errors, and hence accuracy is not improved. See Table 2, where the order $O(h^2)$ is apparent. As expected from the form of ψ, accuracy is not improved when N is increased in the last row of this table.

The same behavior is observed every time that $\psi(\mu, \cdot)$ is a polynomial of degree ≤ 2 in z: for instance, $\psi(\mu, z) = \mu^3(3 + 2\mu z - z^2)$ or $\psi(\mu, z) = (z - 3\mu z^2)\sin\mu$.

(I, N)	$E_{\text{abs}}(Q)$	(μ, z)	order
$(11, 10)$	1.26×10^{-2}	$(-1, 0.88888...)$	
$(33, 10)$	7.55×10^{-4}	$(-1, 0.88888...)$	$\frac{2\ln(\frac{126}{7.55})}{\ln(10)} = 2.447$
$(101, 10)$	7.83×10^{-5}	$(0.8, 1)$	1.967
$(321, 10)$	8.29×10^{-6}	$(0.85625..., 1)$	1.951
$(1001, 10)$	8.72×10^{-7}	$(0.882, 1)$	1.956
$\mathbf{(1001, 901)}$	$\mathbf{9.23 \times 10^{-7}}$	$\mathbf{(0.808, 1)}$	

Table 2: Numerical results for the test case with exact solution $\psi(\mu, z) = \mu^2 z^2$, for $\alpha(\mu, z) = |\sin(12\mu z)|$ and $\sigma(\mu, z) = 1 + \sin(12\mu z)\cos(12\mu z)$.

A complementary case holds every time that $\psi(\cdot, z)$ is a polynomial of degree ≤ 1 in μ. If the exact solution is, let us say, $\psi(\mu, z) = \mu z^3$ or $\psi(\mu, z) = (1 + \mu \cos z) \sin z$, then the order $O(k^2)$ is achieved by increasing N while maintaining I constant. Results for a particular case can be seen in Table 3. Observe that, despite the remarkable refinement of the μ-mesh, the error in the last row does not diminish in a significant way; in other words, accuracy is not improved when I is increased.

(I, N)	$E_{\text{abs}}(Q)$	(μ, z)	order
$(11, 10)$	2.81×10^{-3}	$(-1, 0)$	
$(11, 29)$	2.99×10^{-4}	$(-1, 0)$	$\frac{2 \ln(\frac{28.1}{2.99})}{\ln(10)} = 1.949$
$(11, 91)$	2.90×10^{-5}	$(-1, 0)$	2.025
$(11, 281)$	3.00×10^{-6}	$(-1, 0)$	1.971
$(11, 901)$	2.90×10^{-7}	$(-1, 0)$	2.028
$\mathbf{(1001, 901)}$	$\mathbf{2.87 \times 10^{-7}}$	$\mathbf{(-1, 0)}$	

Table 3: Numerical results for the test case with exact solution $\psi(\mu, z) = \mu z^3$, for $\alpha(\mu, z) = |\sin(12\mu z)|$ and $\sigma(\mu, z) = 1 + \sin(12\mu z) \cos(12\mu z)$.

3.1.3 Test case with known regular solution #3

If the exact solution is

$$\psi(\mu, z) = \ln(2 + \mu^2 + z^3), \tag{26}$$

then the method is not exact with respect to any of the variables, and hence I and N have to be simultaneously increased to improve accuracy with order 2. The comparison between the exact and numerical solutions as well as the order of convergence are shown in Table 4. Table 5, which compares the numerical solution on different meshes, shows that the value of order*, computed from $D_{\text{abs}}(Q)$, is a good indicator of the order.

(I, N)	$E_{\text{abs}}(Q)$	(μ, z)	order
$(11, 10)$	7.05×10^{-3}	$(-1, 0)$	
$(33, 29)$	5.78×10^{-4}	$(-0.0625, 0.17857...)$	$\frac{2 \ln(\frac{70.5}{5.78})}{\ln(10)} = 2.173$
$(101, 91)$	5.87×10^{-5}	$(-0.04, 0.16666...)$	1.986
$(321, 281)$	5.72×10^{-6}	$(-0.04375, 0.15714...)$	2.022
$(1001, 901)$	5.85×10^{-7}	$(-0.04, 0.15888...)$	1.981

Table 4: Numerical results for the test case with exact solution (26), for $\alpha(\mu, z) = |\sin(12\mu z)|$ and $\sigma(\mu, z) = 1 + \sin(12\mu z) \cos(12\mu z)$.

(I,N)	$(2I-1,2N-1)$	$D_{\text{abs}}(Q)$	(μ,z)	order*
$(21,21)$	$(41,41)$	1.11×10^{-3}	$(-0.1,0.2)$	
$(41,41)$	$(81,81)$	2.77×10^{-4}	$(-0.05,0.175)$	$\frac{\ln(\frac{11.1}{2.77})}{\ln(2)}=2.006$
$(81,81)$	$(161,161)$	6.87×10^{-5}	$(-0.025,0.1625)$	2.010
$(161,161)$	$(321,321)$	1.71×10^{-5}	$(-0.025,0.16875)$	2.004
$(321,321)$	$(641,641)$	4.27×10^{-6}	$(-0.03125,0.165625)$	2.002
$(641,641)$	$(1281,1281)$	1.07×10^{-6}	$(-0.03125,0.165625)$	2.0009

Table 5: Numerical results for the test case with exact solution (26), for $\alpha(\mu,z)=|\sin(12\mu z)|$ and $\sigma(\mu,z)=1+\sin(12\mu z)\cos(12\mu z)$.

3.2 Examples from [6], by Kim and Tranquilli

Kim and Tranquilli employ in [6] the Fokker-Planck equation in the 1D slab motivated by the modelling of light propagation in biological tissue. They show some plots that can be used for comparison with our results.

3.2.1 Kim-Tranquilli's problem #1

Problem (55a)–(55c) in reference [6] is considered: $Z_{\text{ini}}=0$, $Z_{\text{fin}}=1$, $\alpha(\mu,z)=0.02$, $\sigma(\mu,z)=0.01$, $f(\mu)=1$, $g(\mu)=2$, $W(\mu,z)=0$. Figure 2 shows that it suffices to take $I\in\{20,21\}$, $N=20$ in order to obtain a good agreement with the graphics in [6]. Numerical experiments performed with finer grids (see Figure 3) allow conjecturing that:

- ψ is continuous on Q.
- $\frac{\partial\psi}{\partial\mu}$ does not exist at $(0,Z_{\text{ini}})$ and at $(0,Z_{\text{fin}})$.
- $\lim_{z\downarrow Z_{\text{ini}}}\frac{\partial\psi}{\partial z}(0,z)=\lim_{z\uparrow Z_{\text{fin}}}\frac{\partial\psi}{\partial z}(0,z)=+\infty$.

As expected from this analysis, convergence of order 2 is not observed and the numerical solution is less accurate, though not bad, near the singularities $\{(0,Z_{\text{ini}}),(0,Z_{\text{fin}})\}$. Inasmuch as order 2 must be seen when the solution is regular, the lack of order 2 supports the idea, as do the plots in Figures 2 and 3, that the solution of this problem is not regular.

Numerical results shown in Table 6 are corroborated by those in Table 7. The quantity $\widehat{E}_{\text{abs}}(Q)$ in Table 7 is comparing the numerical solutions with a reference solution computed for $I=N=2561$, once more by means of the maximum error over the set of common nodes.

(I,N)	$(2I-1,2N-1)$	$D_{\text{abs}}(Q)$	(μ,z)	order*
$(21,21)$	$(41,41)$	3.34×10^{-2}	$(-0.1,0.95)$	
$(41,41)$	$(81,81)$	6.17×10^{-2}	$(-0.05,0.975)$	$\frac{\ln(\frac{334}{617})}{\ln(2)}=-0.89$
$(81,81)$	$(161,161)$	6.47×10^{-2}	$(-0.025,0.9875)$	-0.07
$(161,161)$	$(321,321)$	5.65×10^{-2}	$(-0.0125,0.99375)$	0.19
$(321,321)$	$(641,641)$	5.16×10^{-2}	$(-0.0125,0.996875)$	0.13
$(641,641)$	$(1281,1281)$	4.59×10^{-2}	$(-0.0125,0.9984375)$	0.17

Table 6: Numerical results for Kim-Tranquilli's problem #1.

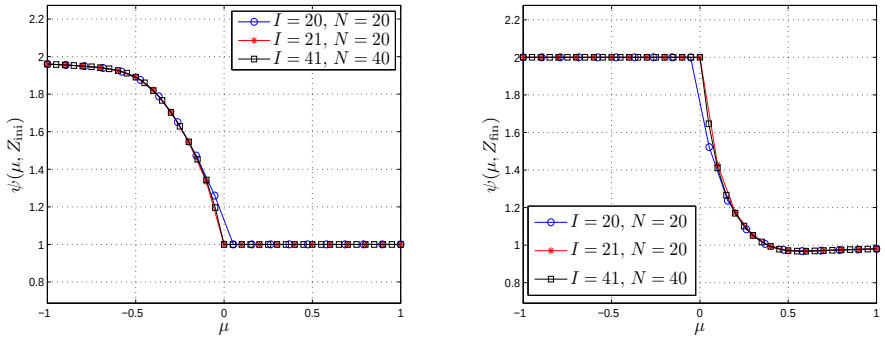

(a) At $z = Z_{\rm ini} = 0$.

(b) At $z = Z_{\rm fin} = 1$.

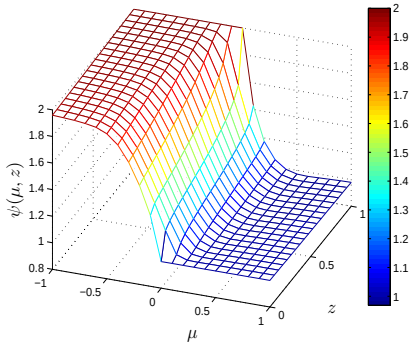

(c) Complete solution for $I = 21$, $N = 20$.

Figure 2: Approximate solution of Kim-Tranquilli's problem #1, obtained with the method of this paper for different meshes.

(I, N)	$\widehat{E}_{\rm abs}(Q)$	(μ, z)	order**
$(21, 21)$	6.48×10^{-2}	$(-0.1, 0.95)$	
$(41, 41)$	9.57×10^{-2}	$(0.05, 1)$	$\frac{\ln(\frac{648}{957})}{\ln(2)} = -0.56$
$(81, 81)$	9.62×10^{-2}	$(0.025, 1)$	-0.008
$(161, 161)$	7.65×10^{-2}	$(0.025, 1)$	0.33
$(321, 321)$	5.52×10^{-2}	$(0.025, 1)$	0.47
$(641, 641)$	4.65×10^{-2}	$(-0.0125, 0.9984375)$	0.25
$(1281, 1281)$	4.11×10^{-2}	$(-0.009375, 0.99921875)$	0.18

Table 7: Numerical results for Kim-Tranquilli's problem #1. $\widehat{E}_{\rm abs}(Q)$ measures the error with respect to a reference solution computed for $I = N = 2561$.

Differences between the even and the odd-scheme. Plots in Figures 2a and 2b show similar results for the even and the odd-scheme. However, there exist remarkable differences in favour of the odd one when the grid is refined. Indeed, results obtained with the even-scheme eas-

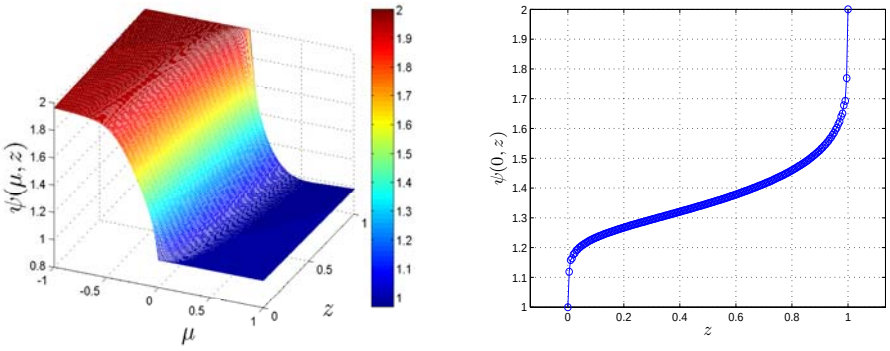

(a) Complete solution. (b) At $\mu = 0$.

Figure 3: Approximate solution of Kim-Tranquilli's problem #1, obtained with the odd-scheme for $I = 201$, $N = 200$.

ily suffer from spurious oscillations near $(0, Z_{\text{ini}})$ and $(0, Z_{\text{fin}})$, and in the worst cases these instabilities propagate along the vicinity of the whole segment $\mu = 0$,[(d)] while none of these problems arise when using the odd-scheme. Figure 4a, which must be contrasted with Figure 3b, manifests this phenomenon. Figure 4b shows that instabilities tend to disappear when refining the z grid. Since $\mu = 0$ is not a node when I is even, the values at $\mu = 0$ have been computed as the arithmetic mean of the values at the nodes $\mu_{\frac{I}{2}} = -\frac{h}{2}$ and $\mu_{\frac{I}{2}+1} = \frac{h}{2}$.

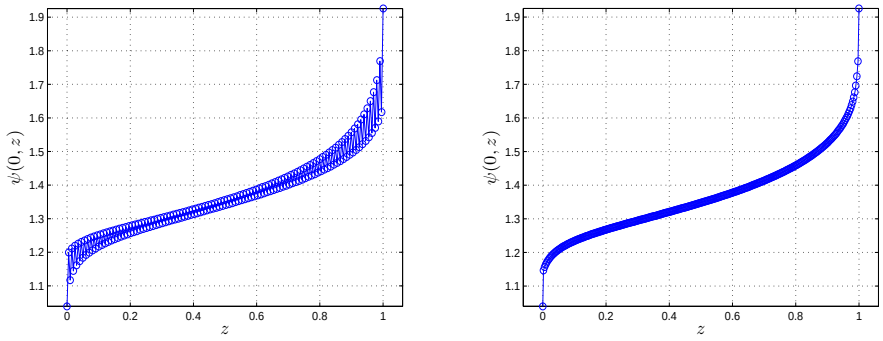

(a) $I = 200$, $N = 200$. (b) $I = 200$, $N = 1200$.

Figure 4: Approximate solution at $\mu = 0$ of Kim-Tranquilli's problem #1, obtained with the even-scheme.

[(d)] These drawbacks of the even-scheme for this problem could be corrected, in all of our trials, by taking $N \sim 6I$.

3.2.2 Kim-Tranquilli's problem #2

Problem (34) with data (57)–(60) in reference [6] is considered: $Z_{\text{ini}} = 0$, $Z_{\text{fin}} = 1$, $\alpha(\mu, z) = 0.01 + 5\text{e}^{-500(z-0.6)^2}$, $\sigma(\mu, z) = \frac{1}{2}(0.01 + 5\text{e}^{-500(z-0.4)^2})$, $f(\mu) = \text{e}^{-100(\mu-1)^2}$, $g(\mu) = 0$, $W(\mu, z) = 0$. Once more, it is not necessary to use a very fine grid ($I \in \{40, 41\}$, $N = 40$ suffices) in order to obtain a good agreement of our Figure 5c with Fig. 5 in reference [6].

As the authors say in [6], this problem models a plane wave normally incident, at $z = 0$, on a plane-parallel slab of tissue having unit thickness. Condition $f(\mu) = \text{e}^{-100(\mu-1)^2}$ is regularizing the plane wave, mathematically modelled with a Dirac delta, by means of a narrow Gaussian, and condition $g(\mu) = 0$ means that no light enters the slab at $z = 1$. The slab of tissue has an absorbing inhomogeneity given by α and a scattering inhomogeneity given by 2σ.

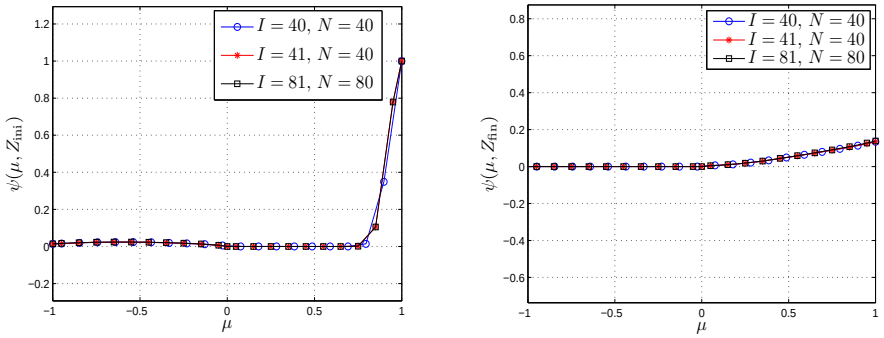

(a) At $z = Z_{\text{ini}} = 0$.

(b) At $z = Z_{\text{fin}} = 1$.

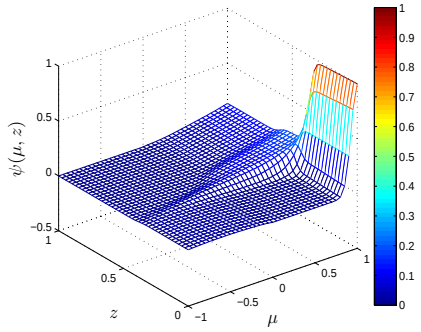

(c) Complete solution for $I = 41$, $N = 40$.

Figure 5: Approximate solution of Kim-Tranquilli's problem #2, obtained with the method of this paper for different meshes. In order to improve visibility, not all values are plotted in (a) and (b).

Spurious oscillations do not occur when solving this problem with the

even-scheme, and the results are comparable to those obtained with the odd-scheme. Tables 8 and 9 report the numerical results. The quantity $\widehat{E}_{\text{abs}}(Q)$ in Table 9 has the same meaning that in Subsection 3.2.1. Notice that the order 2 disappears at the sixth and seventh rows, where round-off errors should not be spoiling yet the approximation. This fact seems to be indicating lack of regularity of ψ to a extent that cannot be specified without further theoretical research. We want to emphasize that by analyzing the order one can get information about the regularity which, as it happens for this problem, might be imperceptible in the graphics.

(I, N)	$(2I-1, 2N-1)$	$D_{\text{abs}}(Q)$	(μ, z)	order*
$(21, 21)$	$(41, 41)$	3.67×10^{-2}	$(1, 0.35)$	
$(41, 41)$	$(81, 81)$	4.23×10^{-2}	$(1, 0.35)$	$\frac{\ln(\frac{367}{423})}{\ln(2)} = -0.20$
$(81, 81)$	$(161, 161)$	1.64×10^{-2}	$(1, 0.3375)$	1.37
$(161, 161)$	$(321, 321)$	3.53×10^{-3}	$(1, 0.3375)$	2.21
$(321, 321)$	$(641, 641)$	7.98×10^{-4}	$(0.0125, 0.003125)$	2.15
$(641, 641)$	$(1281, 1281)$	7.11×10^{-4}	$(0.009375, 0.0015625)$	0.16
$(1281, 1281)$	$(2561, 2561)$	6.33×10^{-4}	$(0.00625, 0.00078125)$	0.17

Table 8: Numerical results for Kim-Tranquilli's problem #2.

(I, N)	$\widehat{E}_{\text{abs}}(Q)$	(μ, z)	order**
$(21, 21)$	9.35×10^{-2}	$(1, 0.35)$	
$(41, 41)$	5.67×10^{-2}	$(1, 0.35)$	$\frac{\ln(\frac{935}{567})}{\ln(2)} = 0.72$
$(81, 81)$	2.06×10^{-2}	$(1, 0.3375)$	1.46
$(161, 161)$	4.24×10^{-3}	$(1, 0.3375)$	2.28
$(321, 321)$	8.50×10^{-4}	$(-0.01875, 0)$	2.32
$(641, 641)$	7.17×10^{-4}	$(0.009375, 0.0015625)$	0.24
$(1281, 1281)$	6.33×10^{-4}	$(0.00625, 0.00078125)$	0.18

Table 9: Numerical results for Kim-Tranquilli's problem #2. $\widehat{E}_{\text{abs}}(Q)$ measures the error with respect to a reference solution computed for $I = N = 2561$.

3.3 Computing time

Table 10 shows the sum of the time employed in defining the matrix and the second member, plus the time spent in solving the linear system. These times rely on a smart MATLAB® implementation.

I	N	time (s)	I	N	time (s)
$\{10, 11\}$	100	$\{0.022, 0.022\}$	$\{100, 101\}$	1000	$\{0.559, 0.537\}$
$\{10, 11\}$	1000	$\{0.083, 0.096\}$	$\{1000, 1001\}$	100	$\{0.614, 0.602\}$
$\{100, 101\}$	100	$\{0.101, 0.095\}$	$\{1000, 1001\}$	1000	$\{15.830, 13.600\}$

Table 10: Values of computing times by using a personal computer with an Intel® Core™ i7-4790 @ 3.60GHz processor.

Ultimately, what one does is to solve a sparse linear system of order $I \times N$, with a degree of sparsity that can be easily derived from the scheme. Hence, there is nothing essentially new in these computing times. We display them so that the reader can immediately judge the scheme's performance in a particular situation. To provide an example, if a refinement $I = 101$, $N = 100$ is good enough for the purposes at hand, then one can solve of the order of 630 Fokker-Planck problems like (1)–(3) in about 1 minute by using a present-day PC.

4 Physical interpretation

The importance of the Fokker-Planck equation (hereinafter FPE) lies in that its solution is an approximation of the solution to the Boltzmann transport equation (BTE) for particles that suffer highly forward-peaked scattering and small energy losses, and the usual examples are charged particles such as electrons or heavy ions.

Both FPE and BTE are equations for the angular flux density of particles, which we denote by ψ in the present paper, and they state the balance between gains and losses for $\boldsymbol{\omega} \cdot \nabla\psi$, the directional derivative of ψ along each direction of propagation $\boldsymbol{\omega} \in S^2$ (here, S^2 is the unit sphere in $\mathbb{R}^3$ and ∇ stands for the gradient with respect to the three spatial variables).

Let $\Omega \subset \mathbb{R}^3$ be the spatial domain. When ψ depends on position $\boldsymbol{x} = (x_1, x_2, x_3) \in \Omega$ only through $x_3 = z$, then $\boldsymbol{\omega} \cdot \nabla\psi = \omega_3 \frac{\partial\psi}{\partial z}$, which corresponds to the first term of Equation (1) if we understand that $\mu = \omega_3$. Under the previous assumption, one says that the problem is posed in the 1D slab if, additionally, the spatial domain has got the form $\Omega = \mathbb{R}^2 \times (Z_{\text{ini}}, Z_{\text{fin}})$ (see Figure 6). The idea is that spatial variables can be reduced from 3 to 1 because of two reasons: ψ does not vary either with x_1 or with x_2, and the domain is a collection of copies of the 1D domain $(Z_{\text{ini}}, Z_{\text{fin}})$.

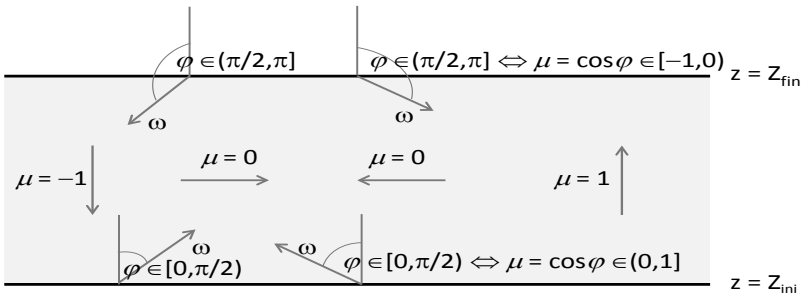

Figure 6: (Section of) the one-dimensional slab. The reader must take into account that this is a special kind of three-dimensional domain.

Notice that

$$\boldsymbol{\omega} = \boldsymbol{\omega}(\varphi, \theta) = (\sin\varphi\cos\theta, \sin\varphi\sin\theta, \cos\varphi) \in S^2,$$

with $\varphi \in [0, \pi]$ the polar angle and $\theta \in [0, 2\pi)$ the azimuthal angle, in the standard spherical coordinate system. Obviously, $\mu = \omega_3 = \cos\varphi$.

When the FPE is posed in the 1D slab, the assumption of *planar-geometry symmetry*, which means that θ-dependence is neglected, is frequently made. Under this new hypothesis, the angular variables reduce from 2 (φ and θ) to 1 (φ or, equivalently, μ) and the operator

$$\frac{\partial}{\partial\mu}\left[\left(1-\mu^2\right)\frac{\partial\cdot}{\partial\mu}\right], \tag{27}$$

which is known as the *continuous scattering operator*, is nothing but the Laplacian over the sphere. Hence, the FPE is imposing for the angle variable the usual diffusive process modelled by the Laplacian.

Equation (1) is the steady monoenergetic FPE in the 1D slab with planar-geometry symmetry, and Equations (2) and (3) are imposing the angular flux density of particles entering the domain (see again Figure 6). In this context, *monoenergetic* means energy-independent.

As it was mentioned in the Introduction, operator (27) does not provide any condition at $|\mu| = 1$. The reason is that the balance expressed by the FPE is enough for getting the angular flux once we know the incoming angular flux through the physical boundary; in other words, the incoming flux boundary conditions suffice to close the FPE. Any attempt to impose the angular flux at interior points (for any direction, not only for $\mu \in \{-1, 1\}$) would result in an overdetermined problem. It is a nice property of the mathematical model that there are also analytical reasons supporting this discussion.

Let us briefly explain, to finish this section, the meaning of the terms in the FPE (1):

1. $\psi(z, \mu)$ is the angular flux density of particles at (z, μ), that is to say, the number of particles, moving from z along direction $\boldsymbol{\omega}(\mu)$, per unit area normal to $\boldsymbol{\omega}(\mu)$, per unit solid angle, per unit energy, and per unit time.
2. The expressions "from z" and "along direction $\boldsymbol{\omega}(\mu)$" in point 1 above must be understood, respectively, as "from (x_1, x_2, z) for any fixed $(x_1, x_2) \in \mathbb{R}^2$" and "along direction

   $$\boldsymbol{\omega}(\mu) = \left(\sqrt{1-\mu^2}\cos\theta, \sqrt{1-\mu^2}\sin\theta, \mu\right)$$

   for any fixed $\theta \in [0, 2\pi)$". No ambiguity arises because our problem is, by assumption, independent of the space variables (x_1, x_2) and of the azimuthal angle θ.
3. $\mu\frac{\partial\psi}{\partial z}$: directional derivative of ψ along direction $\boldsymbol{\omega}(\mu)$.
4. $\alpha\psi$: this term accounts for losses due to absorption, and α is the *absorption coefficient*.

5. $\sigma \frac{\partial}{\partial \mu} \left[\left(1-\mu^2\right) \frac{\partial \psi}{\partial \mu} \right]$: diffusion term modelling the forward-peaked scattering events. Here, $\sigma = \frac{\Sigma_{\mathrm{tr}}}{2}$, where Σ_{tr} is the *momentum transfer* or *transport-corrected scattering cross section*.
6. W: this function represents an internal source of particles wherever it is positive, and an internal sink wherever it is negative.

5 Conclusions

We have presented a new numerical scheme for solving the FPE in the 1D slab with planar-geometry symmetry, including in the FPE a source term W. Several plots and other numerical results that support the validity of this scheme have been shown.

The distinctive features of this scheme are that it has got order 2 in both variables μ and z, and that it allows for coefficients α and σ that can depend also on both variables (μ, z).

Actually, the term "scheme" houses in this paper two schemes, which have been referred to as the even and the odd-scheme because they are exclusively applicable, respectively, to meshes with an even or an odd number of μ-nodes. All numerical results confirm that the second one is preferable.

It has also be seen how the knowledge of the order can be used to gain insight into the regularity of the solution.

We have restricted ourselves to the steady monoenergetic problem, but the scheme can also be used for the time and energy dependent problem after performing discretizations in these variables.

We want to mention, finally, the case in which the planar-geometry symmetry assumption is removed, while 1D slab geometry is maintained. Then ψ depends on (μ, θ, z) and the FPE (1) becomes

$$\mu \frac{\partial \psi}{\partial z} + \alpha \psi - \sigma \left\{ \frac{\partial}{\partial \mu} \left[\left(1-\mu^2\right) \frac{\partial \psi}{\partial \mu} \right] + \frac{1}{1-\mu^2} \frac{\partial^2 \psi}{\partial \theta^2} \right\} = W \tag{28}$$

for $(\mu, \theta, z) \in [-1, 1] \times [0, 2\pi) \times [Z_{\mathrm{ini}}, Z_{\mathrm{fin}}]$. Accordingly, functions f and g in boundary conditions (2) and (3) can depend on (μ, θ). Moreover, as $\theta = 0$ and $\theta = 2\pi$ are defining the same direction $\boldsymbol{\omega}$ for every fixed μ, the periodicity conditions

$$\psi_{|\{\theta=0\}} \equiv \psi_{|\{\theta=2\pi\}}, \quad \left(\frac{\partial \psi}{\partial \theta} \right)_{|\{\theta=0\}} \equiv \left(\frac{\partial \psi}{\partial \theta} \right)_{|\{\theta=2\pi\}} \tag{29}$$

must be imposed as well. Periodicity invites to employ Fourier techniques for reducing the problem (see also [6]). The angular flux can be expressed as a Fourier series $\psi(\mu, \theta, z) = \sum_{k=-\infty}^{\infty} \psi_k(\mu, z) \mathrm{e}^{ik\theta}$, the coefficients of which are given by $\psi_k(\mu, z) = \frac{1}{2\pi} \int_0^{2\pi} \psi(\mu, \theta, z) \mathrm{e}^{-ik\theta} \, \mathrm{d}\theta$. Assume that neither α nor σ depend on θ. Then, it can be easily checked that each ψ_k satisfies

$$\mu \frac{\partial \psi_k}{\partial z} + \alpha_k^\star \psi_k - \sigma \frac{\partial}{\partial \mu} \left[\left(1-\mu^2\right) \frac{\partial \psi_k}{\partial \mu} \right] = W_k \text{ for } (\mu, z) \in Q, \tag{30}$$

with $\alpha_k^\star = \alpha + \frac{\sigma k^2}{1-\mu^2}$ and W_k the k^{th} Fourier coefficient of W, which reduces the problem, once more, to our setting. Notice that, except for $k = 0$, the new "absorption" coefficient $\alpha_k^\star$ depends on μ even when α does not; this is another reason to design numerical methods for the problem with μ-dependent absorption coefficient. Equation (30) must be closed with the incoming flux boundary conditions

$$\psi_k(\mu, Z_{\text{ini}}) = f_k(\mu) \text{ for } \mu \in (0, 1], \tag{31}$$

$$\psi_k(\mu, Z_{\text{fin}}) = g_k(\mu) \text{ for } \mu \in [-1, 0), \tag{32}$$

where f_k and g_k are the k^{th} Fourier coefficients of f and g, respectively.

6 Acknowledgements

This work was co-financed by the European Regional Development Fund (ERDF) and the Xunta de Galicia under the GRC2013-014 grant, and by the Spanish Ministry of Economy and Competitiveness under the MTM2013-43745-R grant. The authors are also indebted to Prof. Arnold D. Kim, from the University of California, Merced, for having generously clarified some queries on his paper [6].

References

[1] Beals, Richard. On an equation of mixed type from electron scattering theory, *Journal of Mathematical Analysis and Applications* **58** (1977) 32–45.

[2] Beals, Richard. Indefinite Sturm-Liouville problems and half-range completeness, *Journal of Differential Equations* **56** (1985) 391–407.

[3] Degond, Pierre; Mas-Gallic, Sylvie. Existence of solutions and diffusion approximation for a model Fokker-Planck equation, *Transport Theory and Statistical Physics* **16** (1987) 589–636.

[4] Fisch, Nathaniel Joseph; Kruskal, Martin David. Separating variables in two-way diffusion equations, *Journal of Mathematical Physics* **21** (1980) 740–750.

[5] Hämmerlin, Günther; Hoffmann, Karl-Heinz (1991) *Numerical Mathematics*. Springer, New York, NY.

[6] Kim, Arnold D.; Tranquilli, Paul. Numerical solution of the Fokker-Planck equation with variable coefficients, *Journal of Quantitative Spectroscopy & Radiative Transfer* **109** (2008) 727–740.

[7] Klaus, Martin; van der Mee, Cornelis Victor Maria; Protopopescu, Vladimir. Half-range solutions of indefinite Sturm-Liouville problems, *Journal of Functional Analysis* **70** (1987) 254–288.

[8] Sheng, Qiwei; Han, Weimin. Well-posedness of the Fokker-Planck equation in a scattering process, *Journal of Mathematical Analysis and Applications* **406** (2013) 531–536.

[9] Stein, Daniel; Bernstein, Ira B. Boundary value problem involving a simple Fokker-Planck equation, *Physics of Fluids* **19** (1976) 811–814.

[10] Vanaja, Venkataraman. Numerical solution of a simple Fokker-Planck equation, *Applied Numerical Mathematics* **9** (1992) 533–540.